Mineral. Soc. Amer. Spec. Pap. **3**, 291–306 (1970).

CHEMICAL EQUILIBRIA AND EVOLUTION OF CHLORIDE BRINES

ABRAHAM LERMAN
Canada Center for Inland Waters, Burlington, Ontario

ABSTRACT

Dissolution of subsurface halite beds by ground water may result in the formation of chloride brines at rates which greatly depend on the physical characteristics of the environment, such as diffusivity in porous media, rate of water flow past the salt bed, and the presence of membranes impermeable to salt. For different sets of limiting conditions, estimated times from 30 to 150×10^6 years are required for the NaCl concentration in the subsurface brine (at 100 m above the salt bed) to attain the value of 90 percent saturation with respect to halite.

Sea water and ground waters of comparable ionic composition may evolve into chloride-rich brines, low in sulfate and carbonates, when the loss of H_2O from the brine is accomplished by: (1) relative enrichment in Ca such that the molar quotient $Ca^{2+}/(SO_4^{2-}+HCO_3^-)$ in the brines becomes greater than 1; (2) precipitation of $CaSO_4$ (and $CaCO_3$) mineral phases. After condition (1) has been fulfilled, process (2) results in continuous depletion of the brine in SO_4^{2-} (and carbonates) and further increase in the Ca^{2+} concentration. Data on 94 subsurface brines (5–290 g/liter dissolved solids) support a thesis of Ca enrichment at the expense of Mg in the brine, and an equilibrium precipitation of $CaSO_4$ minerals. The amount of gypsum or anhydrite formed from subsurface brines in such a process is very small relative to the total amount of sediment.

The composition of the chloride-type ground waters and brines of the Jordan-Dead Sea Valley is controlled by the history of halite dissolution and mixing with a brine of the Dead Sea-type. These brines could not have evolved from dilute ground waters by a simple loss of water and precipitation of calcium sulfate minerals. Thermodynamic models for calculation of the degree of saturation of chloride brines with respect to gypsum, anhydrite and halite produce results compatible with measurements and brine-mineral relationships in nature.

INTRODUCTION

The processes responsible for the formation of brines from more dilute solutions may be broadly classified in the following three major classes:
(I) processes in which water is being removed from the solution (deaquation), (II) processes in which solutions react with the surrounding rocks, and (III) mixing of brines of different composition and concentration. Within each class, processes of more restricted scope may be of either primary or ancillary significance in the formation of a brine. In the tabulation below the primary processes are designated by (*p*), and the ancillary processes by (*a*):

I. DEAQUATION
  1. Evaporation (*p*)
  2. Membrane filtration (*p?*)

II. SEDIMENT-BRINE REACTIONS
  1. Dissolution (*p*)
  2. Precipitation (*a*)
  3. Ion exchange (*a*)
  4. Biological activity (*a*)

III. MIXING (*p*)

Evaporation at the Earth's surface or from the groundwater table and, presumably, membrane filtration effectively removing H_2O from the brine are directly responsible for the increase in the concentrations of dissolved solids. Dissolution of salt beds and, possibly, reactions between HCl-containing solutions of deeper crustal origin and the surrounding rocks can also immediately result in large quantities of solids passing into solution. Mixing of a ground water with some highly saline brine may also be viewed as a primary process of the formation of a new brine.

Precipitation of mineral phases from a solution, ion exchange reactions between the solutions and sediments, and biological activity in the brine and sediments—all these may modify the concentrations of the individual components of a brine thereby contributing to a more or less pronounced change in its chemical nature. Such processes do not substantially increase the brine concentration and these are therefore treated as ancillary, even though their importance in shaping the final composition of the brine may be great.

Precipitation of halite in the course of evaporation of sea water is a well known example of a change in the brine composition (SO_4^{2-}/Cl^- ratio in the brine strongly increases in this process). Ion exchange, interpreted broadly, includes dolomitization reactions in the course of which the brine becomes enriched in calcium and depleted in magnesium. The main facet of the biological activity affecting the dissolved solids contents of brines is the activity of sulfate-reducing bacteria. The bacterial activity is considered responsible for the low sulfate concentrations in certain subsurface (Graf *et al.*, 1966, with a review of earlier literature) and surface brines.

RATES OF BRINE FORMATION

Stratigraphic information on a subsurface brine can in many cases tell a good deal about the age and origin of that brine, yet little can be inferred about the rate at which the brine formed. The picture is somewhat clearer with respect to many brine lakes of approximately known age, from which the minimum rates of the brine formation had been estimated (Langbein, 1961).

Considering the least clear first among the primary processes of the brine formation listed in the preceding section, mixing is likely to be a process of highly variable rates which depend on such factors as the flow rates and volumes of the brine reservoirs.

Membrane filtration, when effective, is a very slow pro-

cess controlled by the water flow rates through poorly permeable beds. In experiments with dilute (under 3%) NaCl solutions effective hyperfiltration through various artificial membranes has been achieved at flow rates on the order of 5×10^{-5} to 5×10^{-4} cm^3/cm^2·sec (Baldwin *et al.*, 1969; Johnson and Harrison, 1969). These flow rates are equivalent to 15 to 150 m/cm^2·yr.

The rate of formation of a brine by surface evaporation and/or dissolution of saline minerals can vary greatly depending on the specific physical conditions of the environment, and any temporary interruptions or reversals in the process. However, limiting rates for these processes can be estimated for certain simplified physical situations, five such situations to be discussed in this section. It will be shown that relatively small changes in the physics of the environment result in great differences in the rates of increase in dissolved solids content of the brines forming by different processes. For the purpose of this illustration the five processes considered below apply to a brine column 100 m deep, containing initially NaCl at the concentration of 0.2 mole/1000 g H_2O (approximately 1% NaCl). The generality of the arguments is not lost by considering a pure NaCl solution rather than a solution containing different ionic species.

Surface evaporation. This is a relatively fast process: the mean global evaporation rate is 0.8–1 m/yr (Harbeck, 1955; Nace, 1967). In warm dry climates the rates are higher by a factor of two, although for a highly concentrated brine the rate of evaporation is lower, being proportional to the difference between the H_2O activity in the brine and the partial vapor pressure of H_2O in the air above it. At the mean rate of 1 m/yr, a 100-m deep column of initial solution (0.2 m NaCl) would be reduced to approximately 5 m in 95 years; at that stage the NaCl concentration in the brine (approx. 5.5 molal) would be 90 percent of its saturation value with respect to halite (6.1 molal) (Fig. 1).

Halite dissolution. In ground waters flowing at very slow rates and dissolving halite, the transport of the Na^+ and Cl^- through the water column may be thought of as controlled by molecular diffusion and advection (*i.e.* flow) of the water mass. Diffusion due to a thermal gradient (the Soret effect) is negligible compared to the molecular diffusion driven by a chemical potential gradient: the Soret coefficients in ionic solutions are approximately three orders of magnitude lower than the molecular diffusion coefficients (Agar, 1959).

The diffusion coefficients of ionic species in water filled porous media are as a rule lower than the diffusion coefficients in bulk aqueous solutions. In the first approximation the value of a molecular diffusion coefficient in a porous medium is lower by a factor of $\sqrt{2}$, the factor arising from geometrical considerations of the diffusional free path in the pore space (Perkins and Johnston, 1963). Experimental determinations of the diffusion coefficients of univalent cations in "moderately crosslinked resins" give values 5 to 20 times lower than the corresponding values in free solutions (Helfferich, 1962, p. 309). The temperature, however, exerts an effect on the diffusion coefficients opposite to that of a porous medium: at 50°C the diffusion coefficients are by a factor of 1.5–3.7 higher than at 25°C (calculated as $D_{50}/D_{25}=\exp[-\Delta E(1/323-1/298)/R]$, for the activation energy of diffusion ΔE in the range 3–10 kcal/mole (Helfferich, 1962)). The concentration dependence of the diffusion coefficient is low for ionic species: the diffusion coefficient of NaCl (at 25°C) increases by less than 8 percent in the concentration range 0.2–5 molal, from 1.475×10^{-5} to 1.59×10^{-5} cm^2/sec (Robinson and Stokes, 1965, p. 515).

A constant value of the diffusion coefficient of NaCl in a "model" brine will be taken as 1×10^{-5} cm^2/sec, and no correction for the difference between the molar and molal concentration scales will be made.

The following four simple cases of a NaCl brine in contact with a halite bed will be considered (Fig. 1):

(i) An "infinitely high" brine column in a porous med-

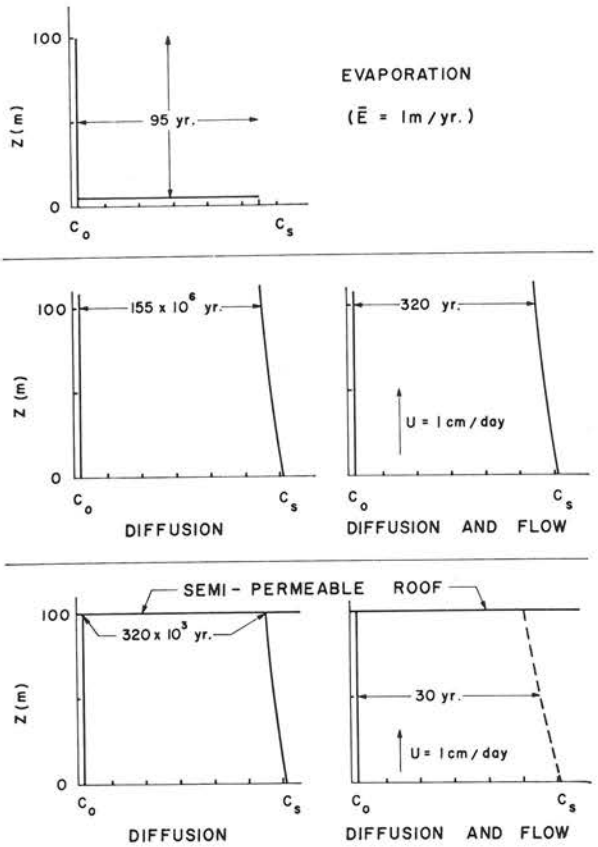

FIG. 1. Rate of increase in the NaCl concentration of 100 m thick brine layer under different conditions. C_o is initial concentration (0.2 molal NaCl); C_s—concentration at equilibrium with halite (6.1 molal). *Top*: concentration increase by evaporation at the mean evaporation rate $\overline{E}=1$ m/yr. *Middle*: transport of dissolved NaCl from a halite bed at $z=0$ upwards by diffusion, and by diffusion and flow; flow rate $U=1\times10^{-5}$ cm/sec (approx. 1 cm/day). *Bottom*: upward transport of dissolved NaCl as in the middle diagram, except for the semipermeable roof at $z=100$ which retains the salt within the brine layer.

ium above an "infinitely" thick halite bed. The initial NaCl concentration in the brine is $C_0=0.2$ m NaCl; the concentration at the brine-bed interface is maintained at the saturation value of halite $C_s=6.1$ m NaCl. At the height $z=100$ m above the brine-bed interface, the position of which in space is considered fixed ($z=0$), the NaCl concentration (C_{100}) would increase as a function of time according to the relationship

$$C_{100} = C_0 + (C_s - C_0)\text{erfc}[z/2(Dt)^{1/2}] \quad (1)$$

where D is the diffusion coefficient of NaCl and t is time (Crank, 1956, p. 33; Carslaw and Jaeger, 1959, p. 63). From relationship (1), the NaCl concentration at 100 m above the interface comes to within 90 percent of the saturation value ($C_{100}=5.5$ m NaCl) in approximately 155×10^6 years. The process is admittedly very slow when molecular diffusion is the sole transporting agent.

The time estimates from relationship (1), as well as (2), (3), and (5), discussed in the following paragraphs, were obtained by trial substitution of different values of t to give the value sought $C_{100}\simeq0.9C_s$. The values of the error function (erf) and error function complement (erfc) were taken from the tables in Carslaw and Jaeger (1959, p. 485), and Abramowitz and Stegun (1964).

(ii) Under the conditions as in (i), the brine flows upwards in the z direction perpendicular to the halite bed. The flow rate is $U=1\times10^{-5}$ cm/sec (approx. 3 m/yr). The equation describing the change in concentration at $z=100$ m above the bed is:

$$C_{100} = C_0 + \tfrac{1}{2}(C_s - C_0)\left\{\text{erfc}\frac{z-Ut}{2(Dt)^{1/2}} + \exp(Uz/D) \times \text{erfc}\frac{z+Ut}{2\sqrt{Dt}}\right\} \quad (2)$$

Relationship (2) is derivable from Carslaw and Jaeger (1959, p. 388) by substituting the following initial and boundary conditions: $C=C_s$ at $z=0$, $t>0$, and $C=C_0$ at $z>0$, $t=0$, which are the conditions of the problem discussed in the present section.

The NaCl concentration at 100 m above the brine comes to $C_{100}=5.5$ molal in approximately 320 years. This is a relatively fast process, and the estimate of 320 years illustrates how a flow rate as low as 1 cm/day can accelerate the increase in the brine concentration by a factor of 5×10^5, compared with an estimate of 155×10^6 years obtained for the case of diffusion without the flow.

(iii) Under the conditions as in (i) a semi-permeable roof is located at 100 m above the brine-halite bed interface keeping all the NaCl diffusing upwards confined to within the 100 m column. This is a fairly realistic assumption, and such physical conditions are likely to be encountered in nature.

The initial and boundary conditions are:

$$C_0 = C \text{ at } 0 < z < l, \quad t = 0;$$
$$C_s = C \text{ at } z = l, \quad t > 0;$$
$$dC/dz = 0 \text{ at } z = 0.$$

The last condition of zero concentration gradient at the upper boundary defines the impermeability of the roof. It should be noted that for mathematical convenience the coordinates in this example have been changed by setting $z=0$ at the upper boundary, and $z=l$ at the brine-bed interface. The distance between the boundaries is $l=100$ m, as before. The appropriate equation for the concentration change at the upper boundary (C_{100}, at $z=0$) as a function of time is (*cf.* Carslaw and Jager, 1959, p. 100):

$$C_{100} = C_s + \frac{4}{\pi}(C_s - C_0)\sum_{n=0}^{\infty}\frac{(-1)^{n+1}}{2n+1}\times \exp\{-Dt\pi^2(2n+1)^2/4l^2\} \quad (3)$$

The time required for C_{100} to attain the value of 5.5 m NaCl, or 90 percent saturation with respect to halite is approximately 320,000 years. An impermeable bed clearly has a pronounced effect on the rate of the brine formation as compared with a much longer time needed to attain the same concentration under the conditions of free diffusion through an upwards unlimited medium considered in case (i).

(iv) This case is a logical extension of case (iii): the roof at 100 m above the halite bed is a semipermeable membrane retaining all the salt but letting the water pass through. The brine flows upwards from the halite bed at the rate of 1×10^{-5} cm/sec. Under such conditions all the NaCl transported from the basal bed upwards is being retained within the 100 m thick brine column. A simple method of estimating the mean NaCl concentration within the brine column is first to assume that no semipermeable roof exists; second, the total amount of NaCl transported by diffusion and flow upwards may then be evaluated by integrating its concentration over the distance from the salt bed ($z=0$) upwards ($z=\infty$): $\int_0^\infty C dz$, where the concentration C in the semiinfinite medium is given by relationship (2); third, the total amount of NaCl added to the brine column over a certain period of time, as obtained by integration of (2), may be divided into the volume 100 m $\times1$ cm^2 to give a mean concentration within the 100 m column.

From (2), the total amount of salt added from the lower boundary into the semiinfinite medium (M, in g/cm^3) is

$$M = \int_0^\infty (C - C_0)dz = (C_s - C_0)\left\{\frac{Ut}{2} + \left(\frac{Ut}{2} + \frac{D}{U}\right) \cdot \text{erf}\frac{U\sqrt{t}}{2\sqrt{D}} + \sqrt{\frac{Dt}{\pi}}\exp(-U^2t/4D)\right\} \quad (4)$$

and the mean concentration of NaCl ($\overline{C}$) in the 100-m layer can be found by dividing M into 10,000 cm and adding to the initial concentration (C_0 in g/cm^3 or moler/cm^3).

$$\overline{C} = C_0 + \frac{C_s - C_0}{10{,}000}\left\{\frac{Ut}{2} + \left(\frac{Ut}{2} + \frac{D}{U}\right)\times \text{erf}\frac{U\sqrt{t}}{2\sqrt{D}} + \sqrt{\frac{Dt}{\pi}}\exp(-U^2t/4D)\right\} \quad (5)$$

Relationship (5) is physically meaningful only for those values of t which make the mean concentration not greater than the saturation value ($\overline{C}\leq C_s$).

Using, as before, vertical flow rate $U=1\times10^{-5}$ cm/sec and diffusion coefficient $D=1\times10^{-5}$ cm^2/sec, substitution

of different values of t into relationship (5) gives, by trial and error, $t \simeq 30$ years as the length of time needed for the mean NaCl concentration to attain the 90 percent level of saturation with respect to halite. Here, as in case (ii), the vertical flow greatly accelerates the rate of brine formation.

It may be noted that at the flow rate of approximately 3.16 m/yr used in the preceding computation, the mean residence time of water in the column is approximately 30 years:

$$\frac{100 \text{ m}}{3.16 \text{ m/yr}} = 30 \text{ yr}$$

Thus it is clear that under the conditions chosen, the vertical flow, rather than diffusion, is the main mechanism of the salt transport. The scale length of the system is $D/U = 1$ cm, a very small number compared to the 100-m long brine column. For the diffusion to contribute significantly to the dispersion of solute in the presence of flow $U = 1$ cm/day, the diffusion coefficient should have been several orders of magnitude greater, making the scale length on the order of meters or tens of meters. Such high values of the diffusion coefficient, however, would fall in the range of turbulent, or eddy, diffusion, which is not a likely dispersion mechanism in a porous rock.

Concentration increase by flow and diffusion, and increase by mixing. Relationship (5) describing the increase in the solute concentration in the brine column above the salt bed may be simplified when long periods of time are considered. For large t the erf term on the right-hand side of (5) approaches 1 and the exponential term tends to 0; when the term D/U is small compared with $Ut/2$, as in the case discussed, the relationship may be written as

$$\overline{C} \cong C_0 + (C_s - C_0)Ut/10^4 \qquad (6)$$

which shows that the rate of increase in the concentration in the brine column is a linear function of t. The relationship is valid for all those values of t as long as the condition $\overline{C} \leq C_s$ is met. Relationship (6) describes essentially a case of "piston flow" where the dilute brine of initial concentration C_0 is made to occupy progressively smaller fraction of the volume $(1 - Ut/10000)$ when it is being displaced due to the inflow of the concentrated brine (C_s) from below, such that the two brines do not mix in the process.

If, however, the concentrated brine (C_s) entering at the salt bed-brine interface undergoes complete mixing with the dilute (C_0) brine within the volume of 100 m$\times$1 cm^2 (*i.e.* the volume of the brine column is maintained constant by the removal of excess water through the semipermeable roof), then the concentration in the brine column increases as:

$$\overline{C} = C_0 + C_s Ut/10^4 \qquad (7)$$

From (6) and (7) it follows that the rate of increase in concentration $(\partial\overline{C}/\partial t)$ is proportional to the concentration difference $\overline{C}_s - \overline{C}_0$ in the case of no mixing ("piston flow"), and to the concentration of the entering brine C_s in the case of complete mixing. The rates are very similar when the initial concentration C_0 is small compared with C_s:

$$(\partial C/\partial t)_{\text{n.m.}}/(\partial C/\partial t)_{\text{m.}} = (C_s - C_0)/C_s \cong 1 \qquad (8)$$

where the subscripts n.m. and m. stand for "no mixing" and "mixing," respectively. When the concentration in the original brine (C_0) is not negligibly small compared with C_s, a "piston flow" will result in the formation of a brine at a lower rate than in the case of complete mixing:

$$(\partial\overline{C}/\partial t)_{\text{n.m.}}/(\partial\overline{C}/\partial t)_{\text{m.}} = (C_s - C_0)/C_s < 1 \qquad (9)$$

In the cases discussed earlier, where the initial concentration value used $C_0 = 0.2$ was much lower than the value in the saturated brine $C_s = 6.1$, the times required for the brine column to attain saturation with respect to halite would be very similar (approximately 30 years) both for the complete mixing case and the case of "piston flow" without mixing.

Chloride Brines and Sulfate Depletion

A large class of brines, in part associated with oil fields and evaporite deposits, is characterized by the predominance of Cl^- among the anions, and Na^+ and Ca^{2+} among the cations. The majority of the chloride brines are commonly thought of as having evolved from sea water and sea water brines entrapped in sediments (Graf *et al.*, 1966; White, 1965; Bentor, 1969), although the origin of some brines can be traced, by the nature of their chemical composition, to the dissolution of rock salt (*e.g.*, Manheim and Bischoff, 1969). As most ground waters and sea water contain sulfate and carbonate in varying proportions in addition to chloride, straight deaquation of a brine would not normally produce a brine highly enriched in chloride. A number of ancillary processes effectively removing sulfate and carbonate species as the concentration of the brine builds up can, however, insure the ultimate low sulfate and carbonate content of a highly saline brine. The commonly invoked ancillary mechanisms are the bacterial sulfate reduction with the concomitant formation of HCO_3^- due to the oxidation of organic matter (*e.g.*, Graf et al., 1966); removal of HCO_3^- (balanced by Na^+) from the brines through subsurface clay membrane filters (Graf *et al.*, 1966; White, 1965), its uptake in the regrading and reconstitution of clay minerals (Mackenzie and Garrels, 1966), and precipitation of $CaCO_3$.

It is the purpose of the present section to show that another mechanism—precipitation of calcium sulfate phases—can be an effective ancillary process which leads to the formation of chloride brines. Calcium sulfates (gypsum and anhydrite) are the only poorly soluble mineral phases which can control the concentration of sulfate in natural brines. If in the original brine the calcium concentration is lower than that of sulfate, then the precipitation of $CaSO_4$ minerals would remove essentially all the calcium from the brine, yet only part of the total sulfate equivalent to the amount of calcium would be removed. The concentration of the remaining sulfate in the brine may continue to increase as the brine looses water. Sea water and many fresh and brackish ground waters are characterized by Ca^{2+}/SO_4^{2-} molar ratio lower than 1, and their progressive deaquation during continuous precipita-

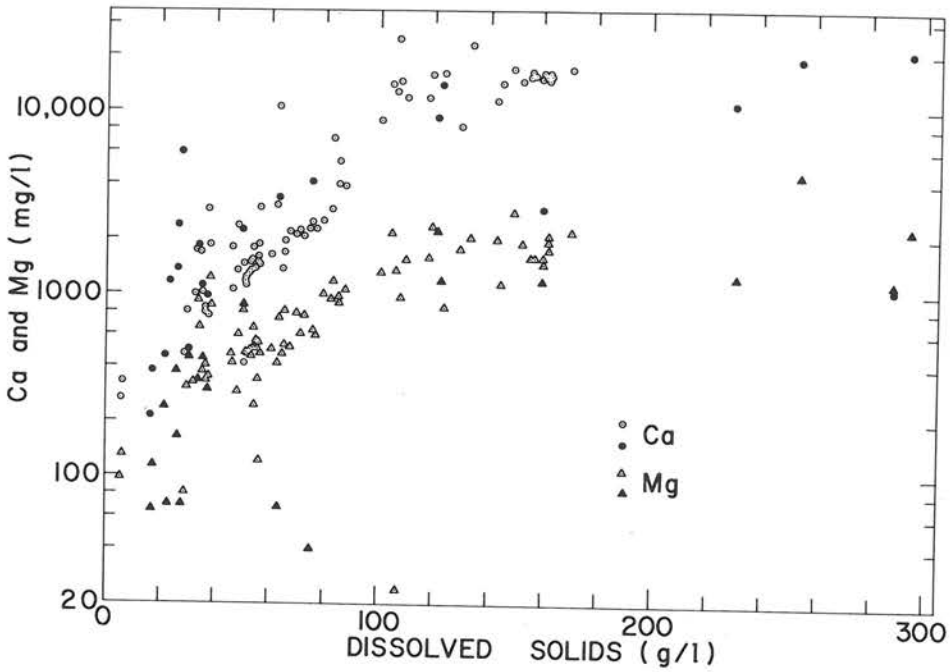

FIG. 2. Calcium and magnesium concentrations in subsurface brines plotted against the concentration of total dissolved solids. Data from White *et al.* (1963)—solid circles and triangles; Table 12, analyses 2–6; Table 13, analyses 1, 2, 3, 5, 6, 10, 12, 13; Table 15, analyses 3, 5, 9; Table 16, analyses 3, 7, 11, 14, 15. These are data from different localities, with the brine density values reported in the tables. From Bentor (1969)—open symbols; Appendix, analyses 1–18, 20–25, 27, 29–36, 38–46, 48–53, 55–78, 82, 83. The larger number of data on subsurface brines from Israel taken from Bentor (1969) as compared with a "worldwide" sample of White *et al.* (1963) is unlikely to introduce a lithological bias insofar as the Iaraeli brines occur in various types of sediment.

tion of gypsum would necessarily result in the sulfate enrichment of the brine. The importance of the Ca^{2+} concentration in determining whether the brine would evolve to either a chloride-sulfate or chloride brine has been recognized by Hutchinson (1957, p. 567–568).

When the removal of HCO_3^- and CO_3^{2-} from the brine is accomplished by $CaCO_3$ precipitation, a similar reasoning applies to the significance of the calcium concentration. Thus it is convenient to consider in brines the molar quotient $Ca^{2+}/(SO_4^{2-}+HCO_3^-)$ which is an indicator of whether a brine can become depleted in sulfate (and carbonates) by precipitation of $CaSO_4$ (and $CaCO_3$) mineral phases. If the quotient is smaller than 1, precipitation of gypsum would not deplete the brine of its sulfate. To achieve the latter the quotient value must be greater than 1. This means that either Ca^{2+} must be added to the brine or SO_4^{2-} and HCO_3^- must be removed from the brine, or both. The processes which may result in the calcium enrichment and sulfate (and carbonate) depletion have been briefly discussed in the introductory section.

To illustrate the possible significance of these processes in the increase of the $Ca^{2+}/(SO_4^{2-}+HCO_3^-)$ quotient values, 94 analyses of subsurface brines containing 5 to 290 g/liter dissolved solids, compiled by White *et al.* (1963) and Bentor (1969), will be considered. The concentrations of Ca^{2+}, Mg^{2+}, SO_4^{2-}, and HCO_3^- (in mg/liter) in those brines were plotted against the total dissolved solids concentration (in g/liter) as shown in Figures 2, 3.

The Ca and Mg data in Figure 2 show that in the brines of less than approximately 30 g/liter dissolved solids the concentrations of the two species are similar. In more concentrated brines, between 30 and 120 g/liter, the Ca^{2+} concentration increases more strongly than Mg. At higher brine concentrations the two alkaline earths slowly increase in approximately the same ratio.

If the relatively smaller increase in the Mg concentration in the brines, as compared with Ca (Fig. 2), were due to incorporation of Mg in silicate minerals then it would be reasonable to find some corroboration of the Mg trend in the HCO_3^- data, as this anion is the one which may be involved in the clay reconstitution reactions (Mackenzie and Garrels, 1966). However, in the absence of any clear trend in the HCO_3^- data (Fig. 3), as well as in the absence of details on the mineralogical and chemical composition of the rocks within which the brines occur, it is more plausible to account for the slower increase in Mg relative to Ca (Fig. 2) as being due to dolomitization reactions between brines and carbonate rocks.

The SO_4^{2-} and HCO_3^- data plotted in Figure 3 scatter greatly, with virtually no individual trends discernible. The diminution of the spread of the individual concentrations in the brines above 120 g/l dissolved solids might be due to the smaller number of samples representative of the high concentration range.

There is little in the sulfate and bicarbonate data of Figure 3 which may support a contention of a reciprocal relationship between the sulfate being reduced and bicarbonate being formed.

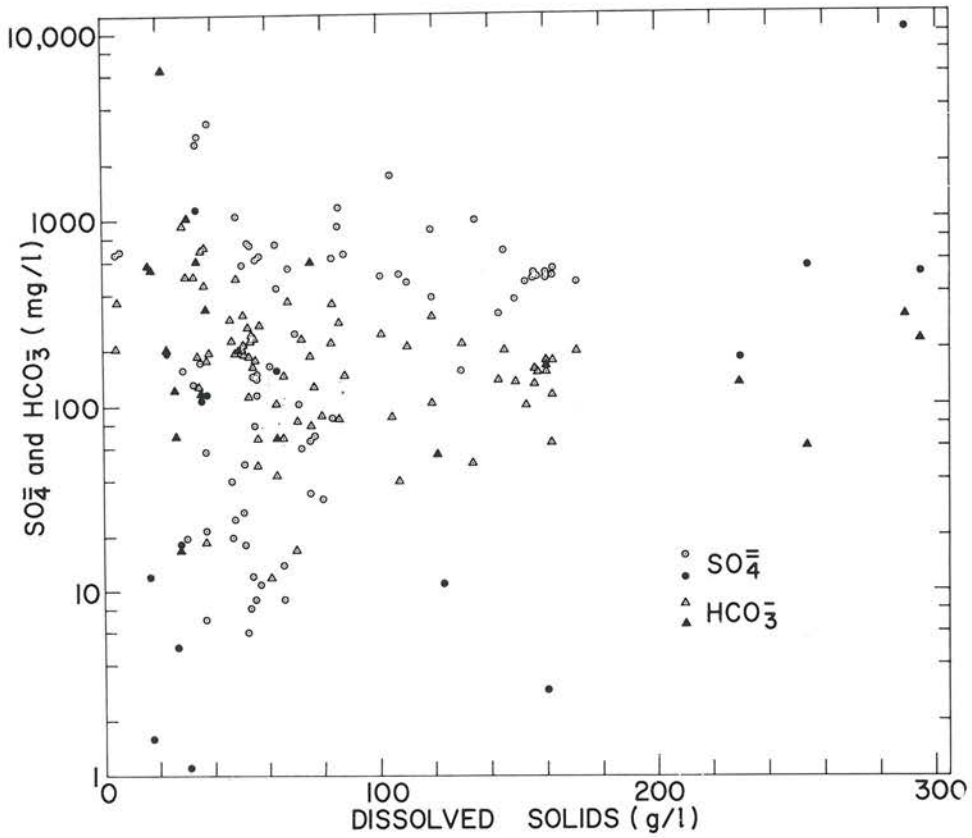

FIG. 3. Sulfate and bicarbonate concentrations in subsurface brines plotted against the concentration of total dissolved solids. Sources of data and symbols as in Fig. 2.

Two parameters were calculated from the analytical data: molar ratio of Ca^{2+} to the sum of SO_4^{2-} and HCO_3^- $[m_{Ca^{2+}}/(m_{SO_4^{2-}}+m_{HCO_3^-})]$, sensitive to the removal of $CaSO_4$ and $CaCO_3$ from the brine, as discussed earlier; and the molar fraction of Ca in the sum of Ca and Mg concentrations $[m_{Ca^{2+}}/(m_{Ca^{2+}}+m_{Mg^{2+}})]$, indicative of any amount of Ca-Mg exchange which might have taken place between the brines and sediments. The values of the $Ca^{2+}/(SO_4^{2-}+HCO_3^-)$ ratio for individual brines plotted in Figure 4 display a trend from the values of near and below 1 in more dilute brines to over 70 in the most concentrated brines.

The composition of the brines as given by the chemical analysis was averaged within successive intervals of 10–20 g/l dissolved solids, and the concentrations of Ca^{2+} and SO_4^{2-} were calculated for each of the "mean" brines at equilibrium with either gypsum or anhydrite at different temperatures. From the calculated concentrations new values of the ratio $Ca^{2+}/(SO_4^{2-}+HCO_3^-)$ were computed, and curves were drawn such as to smooth the calculated values (not shown in the figure). The curve for the anhydrite-brines equilibria at 75°C, shown dashed in Figure 4, fits the scatter of the raw data better than other curves tried for lower temperatures. The temperature of 75°C may be regarded as reasonable for many of the brines occurring at depths 1500–2500 m below the surface.

The concentrations of Ca^{2+} and SO_4^{2-} in brines at equilibrium with gypsum or anhydrite at different temperatures were calculated from the experimentally determined values (Marshall and Slusher, 1968; Marshall, 1967) of the solubility of calcium sulfates and dissociation of the $MgSO_4^\circ$ ion pair in chloride solutions of high ionic strength. The principles of the equilibrium solubility model and method of calculation are summarized in the next section.

The values of the $Ca^{2+}/(Ca^{2+}+Mg^{2+})$ ratio of the brines are shown in Figure 5. The physically meaningful limits of the quotient are 0 (no Ca^{2+}) and 1 (no Mg^{2+}). A gentle upward trend from the ratio value of approximately 0.5 to 0.85 is apparent in the plot of Figure 5. The dashed curve for the anhydrite-brines equilibria in Figure 4 was transferred onto Figure 5 using the calculated values of $m_{Ca^{2+}}$ and the values of $m_{Mg^{2+}}$ from the brine analyses. In this case the fit of the curve for 75°C is also better than for equilibria at lower temperatures.

The proximity of the calculated dashed curves for anhydrite-brines equilibria to the analytical data suggests that the brines above approximately 80 g/l dissolved solids are close to an equilibrium with anhydrite. In the lower concentration range, the points above the dashed curve in Figure 4 represent brines undersaturated with respect to anhydrite: it should be noted that if Ca^{2+} and SO_4^{2-} were added in equivalent amounts to those brines, the values of

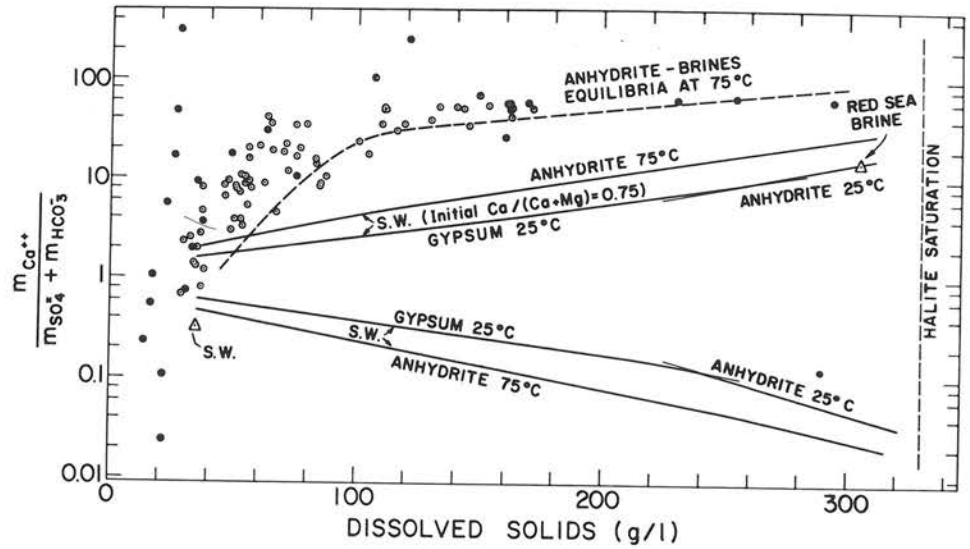

FIG. 4. Molar quotient $Ca^{2+}/(SO_4^{2-}+HCO_3^-)$ in subsurface brines. Solid circles—from data in White *et al.* (1963), open circles—from data in Bentor (1969). The quotient for the Red Sea brine shown for comparison with subsurface data [computed from analyses of Brewer *et al.* (1965) for depths 2105–2155 m. *Discovery* Station 5580]. Curves for equilibria between mineral phases and brines calculated as explained in the text. (S. W.-sea water).

the $Ca^{2+}/(SO_4^{2-}+HCO_3^-)$ quotient, all of which are greater than unity, would decrease falling closer to the dashed curve. In Figure 5, where the same brines are represented by the values of the quotient $Ca^{2+}/(Ca^{2+}+Mg^{2+})$ lesser than unity, addition of Ca^{2+} to the brines would displace the points upwards, closer to the equilibrium dashed curve.

The brines shown in Figures 4 and 5 as a group are likely to have evolved from the left to the right, *i.e.* from the lower to higher concentrations, rather than from right to left, by dilution of some more concentrated brines. Against the latter process it should be noted that simple dilution of a highly saline brine would not have affected the values of the quotients $Ca^{2+}/(SO_4^{2-}+HCO_3^-)$ and $Ca^{2+}/(Ca^{2+}+Mg^{2+})$. In the case, however, of a dilution process when the brine is maintained at equilibrium with either gypsum or anhydrite acting as a very large reservoir of Ca^{2+} and SO_4^{2-}, then the molar quotient $Ca^{2+}/(SO_4^{2-}+HCO_3^-)$ in the brine at low concentrations would approach the value of 1 from above, whereas the quotient $Ca^{2+}/(Ca^{2+}+Mg^{2+})$ would approach 1 from below. Neither of such trends is discernable in Figures 4 and 5.

At this stage two types of brines can be considered; one derived from sea water in which the quotient $Ca^{2+}/(Ca^{2+}+Mg^{2+})=0.15$, and the other from sea water in which part

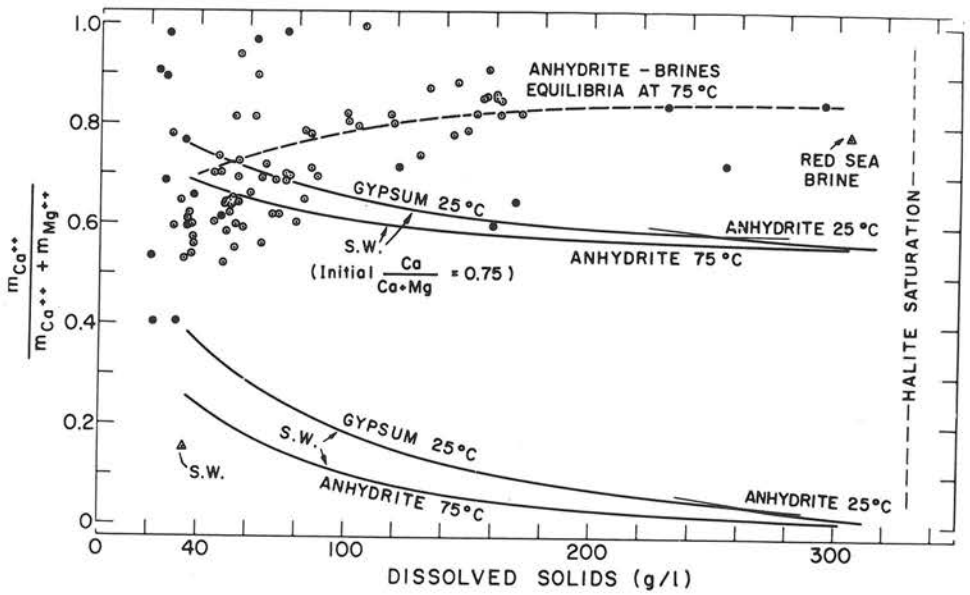

FIG. 5. Molar quotient $Ca^{2+}/(Ca^{2+}+Mg^{2+})$ in subsurface brines. Sources of data and symbols as in Fig. 4.

of Mg had been replaced by Ca to increase the quotient value to 0.75. An ordinary sea water is appreciably below saturation with respect to gypsum, and its equilibration with gypsum at 25°C, or with anhydrite at 75°C, raises the initial values of the two quotients significantly above the point for sea water, as shown in Figures 4 and 5. In the course of progressive deaquation of sea water, when equilibrium with gypsum or anhydrite is maintained, the ratios $Ca^{2+}/(SO_4^{2-}+HCO_3^-)$ and $Ca^{2+}/(Ca^{2+}+Mg^{2+})$ decrease at either 25 or 75°C, as shown by the calculated curves (lower set) for the two solid phases in Figures 4 and 5.

In the case of sea water with part of its Mg replaced by Ca, the initial value of the ratio $Ca^{2+}/(SO_4^{2-}+HCO_3^-)$ is greater than unity. Hence, in the course of deaquation of the brine, the ratio continually increases as Ca^{2+} and SO_4^{2-} are being removed from the solution and calcium sulfate minerals form at equilibrium, as shown by the upper set of solid curves in Figures 4 and 5.

The curves for the two types of sea water brines at equilibrium with calcium sulfate minerals were calculated by increasing the concentrations of the main dissolved species (Na^+, K^+, Mg^{2+}, Cl^-) in proportion to the amount of H_2O removed, and keeping the HCO_3^- concentration constant. The physical significance of the latter constraint is that every X moles of HCO_3^- removed in the process of deaquation of the brine are taken out as $0.5X$ moles of $CaCO_3$ and $0.5X$ moles of CO_2. For such brines the concentrations of Ca^{2+} and SO_4^{2-} at equilibrium with either gypsum or anhydrite were computed using the solubility data of Marshall (1967) and Marshall and Slusher (1968).

In Figure 4, the dashed curve identifying the anydrite-brines equilibria is positioned above a similar curve calculated for the Ca-enriched sea water brines, although the trends of the two curves are analogous. From the relative position of the two curves it may be concluded that a prerequisite for the formation of a chloride brine from sea water (or ground water of comparable ionic ratios) is an increase in the value of the molar quotient $Ca^{2+}/(SO_4^{2-}+HCO_3^-)$ to above 1. Dissolution of $CaSO_4$ minerals by a brine of initial ratio $Ca^{2+}/(SO_4^{2-}+HCO_3^-)<1$ cannot raise the value of the ratio above 1. However, the quotient value may be raised by the addition of Ca at the expense of Mg, as suggested by the data (Fig. 2). The position of the points plotted in Figure 4 also suggests that the process of the relative enrichment in Ca is probably not confined only to the early stages of the brine evolution, but it continues as the brine becomes more concentrated.

If Ca^{2+} and SO_4^{2-} are lost from the brines through precipitation, the gypsum or anhydrite forming in this process should be preserved in the sediment. However, the amounts of the sulfate minerals forming as the concentration of the brine increases are too small to affect the gross mineralogical composition of the sediment. The following example, taken from the data on which Figure 4 is based, illustrates this point: in the course of deaquation of the Ca-enriched sea water from 85 g/l to 165 g/l dissolved solids, the SO_4^{2-} concentration in the brine at equilibrium with anhydrite at 75°C decreases from approximately 0.015 to 0.011 moles/liter. The decrease is equivalent to precipitation of 0.004 moles $CaSO_4$, or 0.54 g anhydrite. Assuming that the porosity of the sediment is of the order of 10–20 percent, 1 liter of brine is distributed through a sediment column of 1 cm^2 in cross-section and 100–50 m in height. Addition of 0.5 g of a mineral to such a sediment column is obviously negligible.

Models of Gypsum, Anhydrite and Halite Solubility in Brines

In view of the importance of the chemical equilibria between brines and saline minerals to the evolution of the brine composition, some simplified models useful in the calculation of the state of saturation of a brine with respect to gypsum, anhydrite and halite will be considered in this section.

Gypsum and Anhydrite. Marshall and Slusher (1968) have shown that the solubility of gypsum and anhydrite in sea water concentrates and other chloride-sulfate type artificial brines may be satisfactorily predicted by a model which takes into account (i) the ionic strength of the solution, and (ii) concentration of the $MgSO_4^\circ$ ion pair in it. Marshall and Slusher (1968) have concluded that $MgSO_4^\circ$ is the most important ion pair which controls the solubility of the calcium sulfate minerals, whereas the existence of the $CaSO_4^\circ$ ion pair is only of minor consequences and it may in general be ignored. Those authors have defined a "practical" ionic solubility product for gypsum and anhydrite expressed in the form:

$$\begin{aligned}\log K_{sp} &= \log(m_{Ca^{2+}} \times m_{SO_4^{2-}}) \\ &= \log K^\circ + 8S\sqrt{I}/(1 + A\sqrt{I}) + BI - CI^2\end{aligned} \tag{10}$$

where K° is the thermodynamic dissociation constant at the specified temperature, S is the Debye-Huckel limiting slope, and A, B and C and empirical constants dependent on temperature. From the definition of $\log K_{sp}$ in relationship (10) it follows that for gypsum at equilibrium with a brine the activity of H_2O is absorbed in the parameters B and C of the solubility equation. The values of K°, A, B, and C have been determined and tabulated by Marshall and Slusher (1968) for gypsum and anhydrite (and calcium sulfate hemihydrate) for a number of temperatures.

For the equilibria between brines and gypsum at 25°C, and between brines and anhydrite at 75°C, considered in the previous section, relationship (10) assumes the following forms:

Gypsum, 25°C:

$$\begin{aligned}\log K_{sp} = &- 4.373 + 8 \times 0.5080\sqrt{I}/(1 + 1.5\sqrt{I}) \\ &+ 0.0194I - 0.0134I^2\end{aligned} \tag{11}$$

Anhydrite, 75°C:

$$\begin{aligned}\log K_{sp} = &- 4.884 + 8 \times 0.5645\sqrt{I}/(1 + 1.575\sqrt{I}) \\ &- 0.020I - 0.0098I^2\end{aligned} \tag{12}$$

In order to calculate the activity product of the Ca^{2+} and SO_4^{2-} ions in a brine, or the concentrations of the two ions at equilibrium with either gypsum and anhydrite, it

is necessary to know the amount of SO_4^{2-} complexed in the ion pair $MgSO_4°$. It can be shown (Marshall, 1967; Marshall and Slusher, 1968) that the concentration of the ion pair may be expressed as

$$(MgSO_4°) = K_{sp}(Mg^{2+})/[(Ca_{eq}^{2+})K_d + K_{sp}] \quad (13)$$

where the parentheses denote molal concentrations, Mg^{2+} is the total magnesium concentration in the brine, Ca_{eq}^{2+} is the calcium concentration at equilibrium with the given calcium sulfate phase, and K_d is the dissociation constant of the $MgSO_4°$ ion pair as determined by Marshall (1967). For the two temperatures considered in the previous section, K_d is given by the following relationships:

$$\log K_d = -2.399 + 8 \times 0.5080\sqrt{I}/(1+\sqrt{I}) \quad (25°C) \quad (14)$$

$$\log K_d = -2.846 + 8 \times 0.5645\sqrt{I}/(1+\sqrt{I}) \quad (75°C) \quad (15)$$

When a brine comes to an equilibrium with either gypsum or anhydrite, equivalent amounts of Ca^{2+} and SO_4^{2-} are either added to, or subtracted from, the brine, depending on whether it is undersaturated or supersaturated with respect to the given mineral. Therefore the ionic solubility product of a calcium sulfate mineral, as in relationship (10), may be written as

$$K_{sp} = (Ca_{eq}^{2+})(SO_{4_{eq}}^{2-}) = (Ca_{or}^{2+} + x) \times (SO_{4_{or}}^{-2} - MgSO_4° + x) \quad (16)$$

where the subscript *or* denotes the molal concentration in the original solution, and x is the number of moles of Ca^{2+} and SO_4^{2-} per 1000 g H_2O added or subtracted from the solution when it comes to an equilibrium with the given mineral. The quantity x may be either positive or negative. Rearrangement of (16) gives a more convenient form:

$$x^2 + x(Ca_{or}^{2+} + SO_{4_{or}}^{2-} - MgSO_4°) + [Ca_{or}^{2+}(SO_{4_{or}}^{2-} - MgSO_4°) - K_{sp}] = 0 \quad (17)$$

from which x can be determined when the remaining quantities are known.

In order to determine the concentration of Ca^{2+} and SO_4^{2-} in a brine at equilibrium with, for example, gypsum at 25°C, the ionic strength of the brine (I) was computed from the chemical analysis, and the quantities K_{sp}, K_d and ($MgSO_4°$) were determined using relationships (11), (13), and (14). In the first calculation of ($MgSO_4°$) the calcium concentration given by the chemical analysis (Ca_{or}^{2+}, in the present notation) was used instead of the unknown Ca_{eq}^{2+}. Next, equation (17) was solved for x and a new value of the ionic strength was computed as:

$$I' = I - 4MgSO_4° + 4x \quad (18)$$

Using the new value of I', equations (11), (13), (14), (17), and (18) were solved again, and the entire procedure was repeated three or four times until the new value of I' differed from the previous value by less than 0.5 percent. The values of x obtained by this procedure were algebraically added to the concentrations of Ca^{2+} and SO_4^{2-} given by the chemical analysis.

Halite. The solubility of halite markedly depends on the concentration and nature of other ionic solutes present. In Figure 6 are shown the effects on the solubility of halite due to some common dissolved components of natural brines. The solubilities shown in Figure 6 are at 25°C, although essentially the same picture holds at higher and lower temperatures, as the solubility of halite varies only little at temperatures below 100°C. Insofar as the solubilities of halite in the presence of either divalent metal chlorides or univalent metal chlorides (Fig. 6) are very different, it may be intuitively concluded that a satisfactory and sufficiently general model of the halite solubility in chloride brines should take into account the concentrations of the individual dissolved components of the brine. Such a model may in fact be based on the so-called Harned's rule (Harned and Owen, 1958, pp. 602–632; Robinson and Stokes, 1965) which describes the dependence of the mean activity coefficients of strong electrolytes in solutions also containing other dissociated solutes.

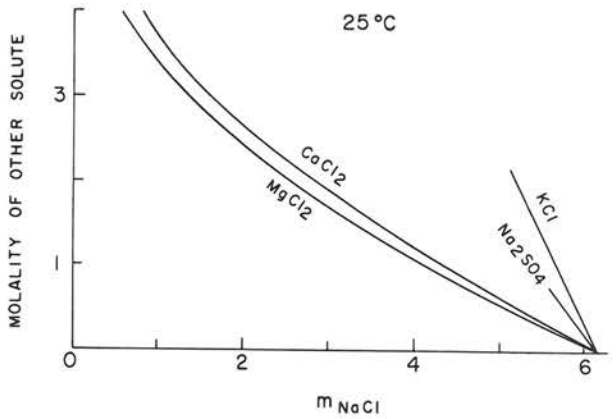

FIG. 6. Solubility of halite in the presence of some other electrolytes at 25°C. Data from averaged solubilities in Zdanovskii *et al.* (1953).

In Harned's rule notation the mean activity coefficient ($\gamma_\pm$) of a strongly dissociated electrolyte, such as NaCl, is given by a relationship of the following type:

$$\log \gamma_{\pm NaCl} = \log \gamma_{\pm NaCl(0)} + \alpha_{1i}\omega_i m_i + \alpha_{1j}\omega_j m_j + \cdots \quad (19)$$

where $\gamma_{\pm NaCl(0)}$ denotes the mean activity coefficient of NaCl in a pure solution containing only NaCl at the same ionic strength as the mixed solution; α_{1i}, α_{1j}, etc., are empirical parameters (Harned's rule coefficients); ω is the ionic strength factor ($\omega=1$ for a NaCl-type electrolyte, $\omega=3$ for $MgCl_2$-type); and m is the molality of the other electrolyte. The coefficients α_{12} are in general characteristic of the specific pair of solutes and they are independent of the presence of other solutes in solution. The relationship for the mean activity coefficient of a strong electrolyte as given by (19) is an approximation. A number of systems (of little geochemical interest, however) are known in which the mean activity coefficient is expressed as a power series in m, where additional terms of the type βm^2 are added to the right-hand side of (19).

From relationship (19) it is clear that the mean activity

coefficient of an electrolyte in a mixed solution can be calculated only for those ionic strengths for which the pure solutions exist and the values of $\gamma_{\pm 1(0)/NaCl(0)}$ are available. Thus, pure NaCl solution becomes saturated with respect to halite at near 6.1 molal NaCl ($I=6.1$), whereas ionic strengths much higher than that may obtain in mixtures of NaCl and $MgCl_2$. This difficulty in obtaining the values of $\gamma_{\pm NaCl(0)}$ for the ionic strengths in the supersaturation region of a pure NaCl solution is circumvented by the use of the mean activity coefficients of HCl which are simply related to the mean activity coefficients of such solutes as NaCl and KCl (Åkerlöf, 1937; Harned and Owen, 1958, p. 617):

$$\log (\gamma_{\pm NaCl(0)}/\gamma_{\pm HCl(0)}) = -0.088I \tag{20}$$

By rearrangement,

$$\log \gamma_{\pm NaCl(0)} = \log \gamma_{\pm HCl(0)} - 0.088I \tag{21}$$

The mean activity coefficients of HCl in aqueous solutions are available up to the ionic strength of 16 (Åkerlöf and Teare, 1937; Harned and Owen, 1958, p. 751), and from relationship (21) it is possible to calculate the mean activity coefficients of NaCl in its pure solutions of concentrations higher than the halite saturation. In this procedure it is assumed that relationship (21) holds for supersaturated NaCl solutions.

Before discussing in more detail the nature and methods of derivation of the α_{12} coefficients, their usefulness in the solution of the following common problems may be restated. For a chloride brine of a known composition the mean activity coefficient of NaCl may be determined by relationship (19) and then the value of the ionic activity product (IAP_{NaCl}) in the brine may be computed as follows:

$$IAP_{NaCl} = a_{Na^+}a_{Cl^-} = m_{Na^+}m_{Cl^-}\gamma^2_{\pm NaCl} \tag{22}$$

Likewise, the NaCl concentration in a brine at equilibrium with halite may be determined from the basic relationship:

$$K_{hal} = m_{Na^+}m_{Cl^-}\gamma^2_{\pm NaCl} \tag{23}$$

In the relationship (23) m denotes the molalities of the Na^+ and Cl^- ions at equilibrium with halite. Specific examples of such a calculation by successive iterations have been described elsewhere (Lerman, 1967).

The coefficients α_{12} for various systems have been determined from the results of isopiestic measurements of vapor pressure over solutions and by the measurements of the individual ionic activities using ion-sensitive reversible electrodes (Lanier, 1965; Platford, 1968; Butler and Huston, 1967; Wu *et al.*, 1968). A different method for the determination of α_{12} from the solubility data, such as those shown in Figure 6, has been described by Åkerlöf (1934). In this method the mean activity coefficient of NaCl in solutions containing NaCl and another solute at equilibrium with halite is determined for a number of different compositions using relationship (23), and the coefficient α_{12} is then calculated from each value of $\log \gamma_{\pm NaCl}$ using relationship (19). When the variation between the different values of α obtained is not large, a mean value of α may be used for the entire range of ionic strength. Although this method is sensitive to the accuracy with which the composition of the solutions at equilibrium with halite has been determined, its advantage is that α_{12} values can be determined for very high ionic strengths.

Table 1 summarizes the value of α_{12} coefficients reported recently by some investigators, as well as the values calculated from solubility data and used in this work.

Although the differences between the values of α_{12} obtained by different methods are appreciable, it may be pointed out that if the values of α_{NaCl-i} other than those given in the last column of Table 1 were used in the calculation of IAP_{NaCl} in the Dead Sea brines (Fig. 8), the agreement between the electrometric measurements and calculated results would not have been nearly as good. This in particular holds for the coefficient $\alpha_{NaCl-MgCl2}$, as $MgCl_2$ is one of the main components of the Dead Sea brines.

For a chloride brine containing NaCl, $MgCl_2$, KCl, $CaCl_2$, and Na_2SO_4 as the main dissolved components (Lerman, 1967; Lerman and Shatkay, 1968), the activity product of the Na^+ and Cl^- ions in the brine may be written, using the values of α_{12} from Table 1, relationships (19) and (21), in the following form:

$$\begin{aligned}\log IAP_{NaCl} &= \log (m_{Na^+}+m_{Cl^-}) + 2\log \gamma_{\pm NaCl} \\ &= \log [(m_{NaCl}+2m_{Na_2SO_4}) \times \\ &\quad (m_{NaCl}+m_{KCl}+2m_{MgCl_2}+2m_{CaCl_2})] \\ &\quad +2(\log \gamma_{\pm HCl(0)} - 0.088I + 0.054m_{MgCl_2} - 0.0134m_{KCl} \\ &\quad +0.0285m_{CaCl_2} - 0.075m_{Na_2SO_4})\end{aligned} \tag{24}$$

In relationship (24) the value of $\gamma_{\pm HCl(0)}$ is taken at the ionic strength I of the brine.

Setting $IAP_{NaCl}=K_{hal}$ in (24), the equation may be

TABLE 1. HARNED'S RULE COEFFICIENTS (α_{12}) AT 25°C FOR NaCl IN SOME SYSTEMS CONTAINING TWO ELECTROLYTES

NaCl-$MgCl_2$

I	1	2	3	4	5
1	0.0146	0.016	0.016	0.019	
3	0.0104	0.011	0.012	0.011	
5			−0.0022	0.008	
6	0.0060	0.009	−0.0004	0.007	
6.8–14.0					0.018

NaCl-$CaCl_2$

I	1	3	6	5
1	0.0040	0.010	0.0092	
3	0.0020	0.000	0.0018	
6	−0.0013	−0.004	−0.0016	
7			−0.0020	
6.9–12.9				0.0095

NaCl-Na_2SO_4

I	1	4	7	5
1	−0.0605	−0.045	−0.0453	
3	−0.0537	−0.045	−0.0490	
6	−0.0500	−0.045		
6.7–7.7				−0.025

NaCl-KCl

I	8	5
1	−0.0235	
3	−0.0235	
6	−0.0275	
6.7–7.7		−0.0134

1. Lanier, 1965; 2. Platford, 1968, 3. Butler and Huston, 1967; 4. Wu *et al.*, 1968; 5. This work; 6. Robinson and Bower, 1966; 7. Butler *et al.*, 1967; 8. Robinson, 1961.

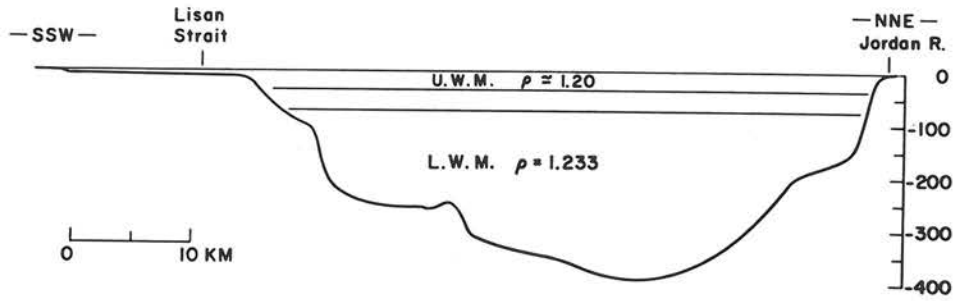

FIG. 7. Cross section of the Dead Sea basin showing the density stratification into the lighter upper water mass and denser lower water mass. Pronounced density gradient exists between the upper and lower water mass. Water depth scale on the right is in meters. Data from depth contour map in Neev and Emery (1967, p. 10).

used to compute the NaCl concentration in brines at equilibrium with halite. In this procedure the value of K_{hal} affects the value of m_{NaCl} obtained. Literature values of K_{hal} (some quoted in Lerman and Shatkay, 1968) differ by as much as 10 percent; therefore, depending on the value of K_{hal} taken, m_{NaCl} computed from (24) may vary by approximately 5 percent.

Application of relationship (24) to the evaluation of the ion activity products and the Na^+ and Cl^- concentrations at equilibrium with halite will be demonstrated in the next section.

CHLORIDE BRINES OF THE JORDAN—DEAD SEA RIFT VALLEY

The Jordan River—Dead Sea Rift Valley is a northern extension of the East African and Red Sea Rift Valley system. The Dead Sea and the saline ground waters in the Jordan—Dead Sea Valley constitute an excellent example of a suite of chloride brines in the range from dilute ground waters to brines precipitating halite. The more salient geological features of the Jordan-Dead Sea Rift Valley which bear on the composition of the ground brines are: (1) calcareous rocks forming the western escarpment of the rift valley; ground waters issuing along the western escarpment have a history of flow through the aquifers in calcareous rocks; (2) occurrence of numerous gypsum, anhydrite and halite beds, and salt structures in the older fill of the rift valley (Neev and Emery, 1967). The most pronounced and conspicuous salt structure is the partly exposed salt dome of Mount Sodom on the southwestern shores of the Dead Sea. The older gypsum, anhydrite and halite beds in the Dead Sea Valley sediments may be of local importance in the control of the composition of some of the saline springs as will be discussed in the following sections.

Present state of the Dead Sea brines. The cross-section of the Dead Sea in Figure 7 shows a pronounced density stratification of the water column. The stratification is apparently "permanent." The bottom sediment of the Dead Sea has been reported as made of halite, occurring below the 40-m water depth line. Thin discontinuous (0–40 cm) layer of detrital material, calcium sulfate and carbonate minerals, covers the halite on the bottom (Neev and Emery, 1967).

Measurements of the activity of the sodium and chloride ions in the Dead Sea brine samples taken at various depths throughout the water column (Lerman and Shatkay, 1968) have shown (Fig. 8) that the less saline upper water mass

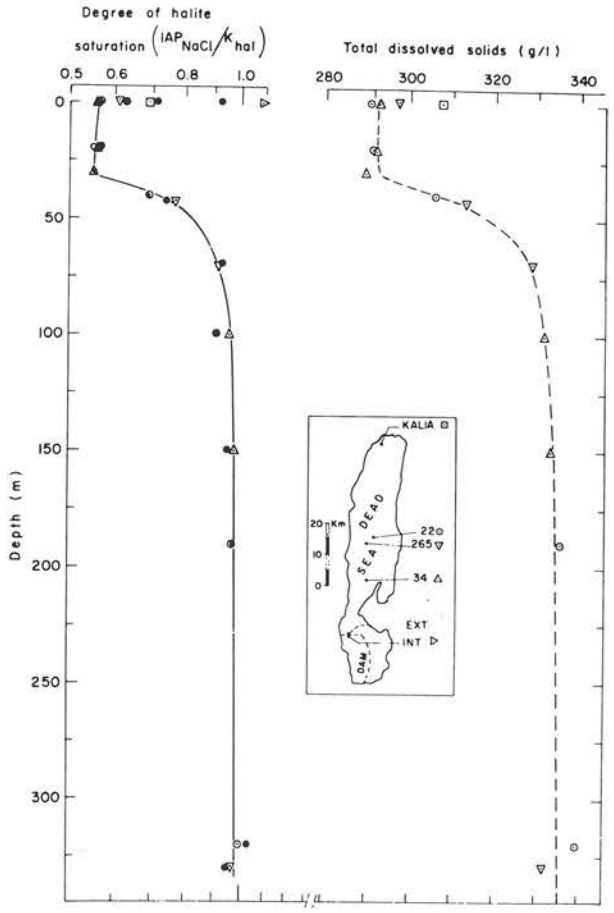

FIG. 8. Degree of brine saturation with respect to halite and total dissolved solids in the Dead Sea brine column. Open symbols refer to station numbers identified in the inset. Solid symbols —degree of saturation calculated from chemical analyses; open symbols—from electrode measurements in Lerman and Shatkay (1968). At station INT t.d.s. = 365 g/l.

(0–35 m) is appreciably undersaturated with respect to halite. The degree of saturation of the brine with respect to halite was expressed as the ratio

$$IAP_{NaCl}/K_{hal} = a_{Na^+}a_{Cl^-}/K_{hal} \quad (25)$$

where IAP_{NaCl} is the ionic activity product of the sodium and chloride ions in the brine as measured with a pair of sodium and chloride ion sensitive electrodes (details of the technique have been described by Lerman and Shatkay, 1968), and K_{hal} is the thermodynamic equilibrium product of the sodium and chloride ions in a solution at equilibrium with halite (at 25°C $\log K_{hal} = 1.581_4$). The value of the $IAP/K = 1$ corresponds to the case of brine saturated with respect to halite. Values lower than 1 represent undersaturation, and values above 1, supersaturation.

It should be noted that the agreement between the measured and calculated values of the degree of halite saturation shown in Figure 8 does not depend on the value of K_{hal} taken: the same K_{hal} is divided into each measured and calculated value of IAP_{NaCl}, as in (25).

In the upper water mass of the Dead Sea the degree of saturation with respect to halite is in the range 0.55–0.7 (Fig. 8). The surface brine sample near saturation, labelled INT in the insert of Figure 8, was taken from a shallow section of the Dead Sea dammed off several years ago in order to increase the rate of evaporation of the brine utilized in an industrial process of carnallite recovery. At present halite forms on the bottom of the dammed section, and the slight supersaturation measured in that brine is compatible with the process observed.

The Dead Sea brine column below approximately 75 m depth is very close to saturation with respect to halite, as shown by the measured (and calculated) points close to the value $IAP/K = 1$ in Figure 8. The absence of any pronounced salinity gradient in the lower water mass (right-hand part of Fig. 8) suggests that it is relatively well mixed. The homogeneous salinity profile agrees well with nearly the same degree of halite saturation in the brine observed between 75 m and 330 m depth. The near saturation with respect to halite in the lower water is in good agreement with the reported occurrence of halite on the Dead Sea floor.

From the known chemical composition of the brines (Lerman and Shatkay, 1968) the values of the IAP_{NaCl} were computed using the thermodynamic model given by relationship (24).

The agreement between the measured and calculated values of the ionic activity product $IAP_{NaCl} = a_{Na^+}a_{Cl^-}$ plotted in Figure 8 (open symbols and solid dots) is as a whole very satisfactory, and it is a test of the validity of the model used in the computation of the IAP_{NaCl} values for the Dead Sea brines.

Historical Note on the Composition of the Dead Sea Brine. Antoine Laurent Lavoisier was the first to analyze the Dead Sea brine in 1778 (analysis cited in Herapath and Herapath, 1849). His results, however, reporting the density and concentration of the calcium and magnesium chloride (combined) and sodium chloride, are far off what may be considered even a crude approximation to the composition of the Dead Sea brine. Throughout the nineteenth century many chemists, geologists and explorers have analyzed the Dead Sea brine, some of the names retaining the historical

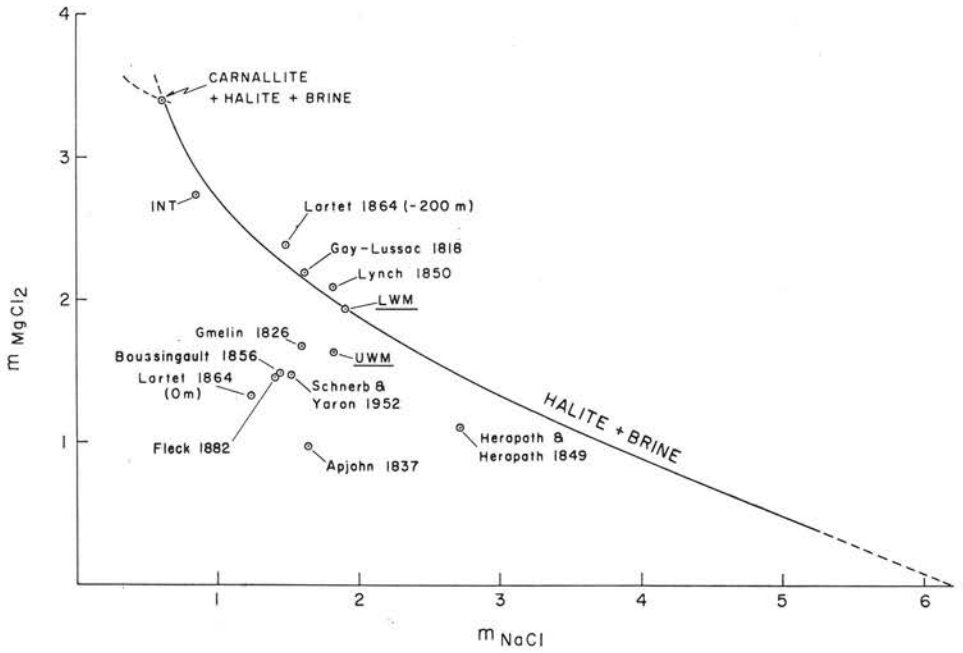

FIG. 9. Some 19th and 20th century results of the determination of the Dead Sea brine composition plotted as the NaCl and $MgCl_2$ molal concentrations. Analyses of Gay-Lussac, Gmelin and Apjohn cited in Herapath and Herapath (1849). Compostion of the upper (UWM) and lower water mass (LWM) from analyses in Neev and Emery (1967). Derivation of the halite-brine and halite-carnallite-brine equilibrium curves discussed elsewhere (Lerman, 1967).

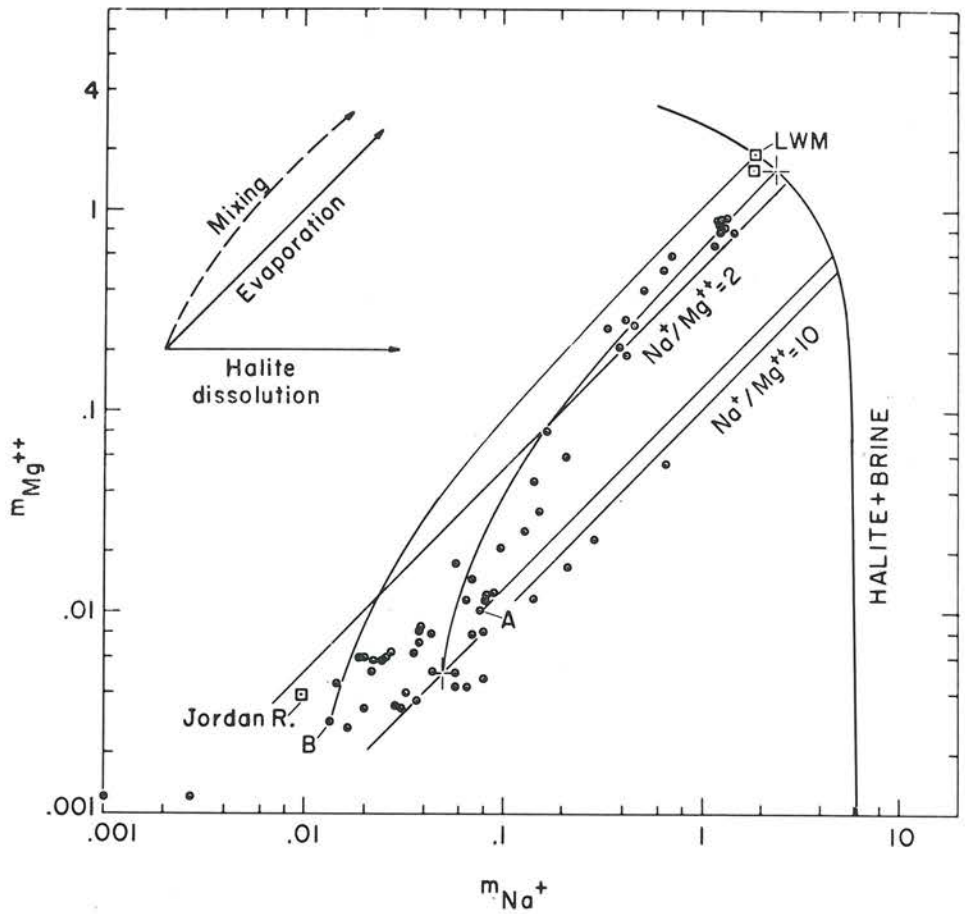

FIG. 10. Changes in the Na^+ and Mg^{2+} content of dilute brines due to dissolution of halite, evaporation or mixing with Dead Sea brines. Open circles: ground waters and saline springs from the southwestern Dead Sea Valley (analyses in Mazor *et al.*, 1969).

memory and prominence even in modern times (Gmelin, Gay-Lussac). A number of analyses (not all) of the Dead Sea brine published in the 19th and 20th centuries are plotted in Figure 9 in terms of the two main components of the brine: NaCl and $MgCl_2$. All of the points plotted, unless specifically indicated, represent the surface water of the Dead Sea. The first chemical analyses confirming the density stratification of the Dead Sea were published by the French geologist Louis Lartet (1864), although the concentrations of the dissolved components in the deep water reported by him seem questionable. The analyses plotted in Figure 9 should be compared with the curve labelled Halite +Brine: the curve gives the composition of the brines at equilibrium with halite at 25°C, when the brines contain the major dissolved components ($MgCl_2$, KCl, $CaCl_2$, and Na_2SO_4) in the same proportions as the Dead Sea lower water mass. Thus the curve gives the NaCl molality at equilibrium with halite in the brines more dilute or more concentrated than the Dead Sea brine. The details of the computational procedure for the halite-brine equilibrium curve have been described elsewhere (Lerman, 1967). The position of the surface water analyses reported by Gay-Lussac in 1818 (Cited in Herapath and Herapath, 1849) and Lynch (1850) near the halite-brine equilibrium curve probably reflects analytical difficulties rather than the absence of density stratification in the early 19th century Dead Sea. The point INT shown in Figure 9 refers to the evaporating brine in the dammed section of the lake discussed earlier. Its position shows that the evaporation has progressed more than half-way to the brine in which carnallite ($KMgCl_3 \cdot 6H_2O$) begins to form.

Modes of the brines formation. In an earlier section it was shown how the enrichment of the brine in Ca relative to Mg and subsequent precipitation of calcium sulfate minerals may result in the formation of a chloride-rich brine. The ground waters and springs in the Jordan-Dead Sea Valley, containing dissolved solids from approximately 0.2 g/liter and up, are characterized by the predominance of chloride over other anions (analyses in Bentor, 1969; Mazor and Mero, 1969; Mazor *et al.*, 1969). As these waters occur within the Dead Sea drainage basin, their chemical composition may be viewed as bearing to a greater or lesser extent on the chemical composition of the Dead Sea water, or vice versa. The possible modes of evolution of the Dead Sea Valley brines, taken as a group, will be first considered in terms of the two main cations: Na^+ and Mg^{2+}. The NaCl and $MgCl_2$ content of a dilute brine plotted as a point in the coordinates representing the NaCl and $MgCl_2$ concentration would change along a path which depends on whether the brine is dissolving halite, undergoing evaporation, mixing with a more concentrated brine, or any combination of these processes. The chemical paths along which the brine may evolve are schematically shown in the upper left of Figure 10. Halite dissolution does not affect the Mg

content of the brine, whereas its Na content increases, displacing the brine to the right in the coordinates of Figure 10. Evaporation of the brine increases the concentration of both Na^+ and Mg^{2+} but does not change the Na^+/Mg^{2+} molal ratio as long as the brine is undersaturated with respect to halite. In the log-log coordinates of Figure 10 this is represented by a straight line the slope of which is constant and determined by the initial Na^+/Mg^{2+} ratio. Mixing of the dilute brine with a more concentrated brine of a different Na^+/Mg^{2+} ratio is represented by a curvilinear plot; the curvature of the mixing line depends on the relative position of the two brines in the Na^+—Mg^{2+} coordinates, or, in other words, on the difference in the Na^+/Mg^{2+} ratio between the two brines.

Bearing these simple relationships in mind, near seventy ground waters and brines from the southwestern part of the Dead Sea Valley, the Jordan River, and the Dead Sea brine (lower and upper water mass) were plotted in Figure 10. The halite-brine equilibrium curve, shown in Figure 9, was transferred to the log-log coordinates of Figure 10. Two straight lines, labelled $Na^+/Mg^{2+}=2$ and $Na^+/Mg^{2+}=10$, were drawn to bracket two hypothetical cases of evaporation of dilute brines such that the values of the Na^+/Mg^{2+} ratio taken were close to the lower and upper limit recorded for the brines. Two curves representing mixing were drawn for the cases of (i) a dilute brine (point B) mixing with the lower water mass of the Dead Sea, and (ii) a brine similar to ocean water (lower cross in Figure 10; approximately 0.5 molal Na^+ and 0.05 molal Mg^{2+}) mixing with a hypothetical brine at equilibrium with halite, of composition only slightly different from the lower water mass (upper cross).

The scatter of the brine data, taken as a group, suggests that no single process could have been responsible for the shaping of their Na^+ and Mg^{2+} content. The brines in the lower concentrations range in Figure 10 suggest that dissolution of halite from the sediments and some deaquation are primarily responsible for the trend in the scatter from the lower left to the right. The higher concentrations are likely to be due to mixing of the more dilute with more concentrated brines in the subsurface, similar in their composition to the Dead Sea brines. The curvilinear trend

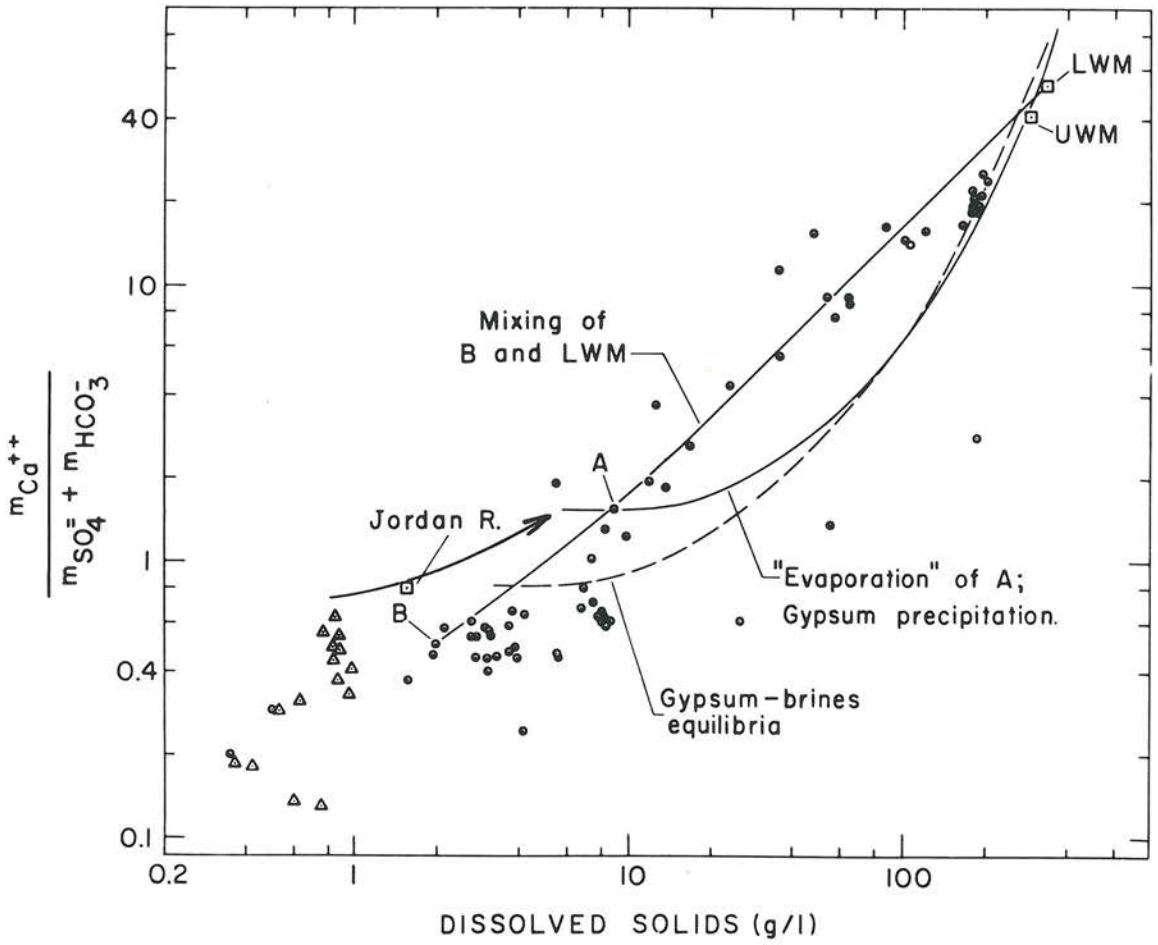

FIG. 11. Changes in the molar quotient $Ca^{2+}/(SO_4^{2-}+HCO_3^-)$ in dilute brines due to mixing with Dead Sea brines, and due to evaporation with concomitant precipitation of gypsum. Circles—Dead Sea Valley brines (analyses in Mazor *et al.*, 1969); triangles—upper Jordan Valley, Lake Tiberias area (analyses in Mazor and Mero, 1969).

of the scatter of data in the higher concentration range supports this conclusion.

The mixing of the dilute and (hypothetical) subsurface brines similar to the Dead Sea brine, inferred from the analysis of the concentration of the two major components (NaCl and $MgCl_2$), is in good agreement with the conclusions of Gat (Gat *et al.*, 1969), based on the isotopic composition of the brine water and the total salt content, regarding the contribution of the Dead Sea brines to the composition of the more saline spring waters (0.2–1 molal Na^+) plotted in Figure 10.

The mixing of the ground waters with the subsurface brines of the Dead Sea type is further strengthened by the distribution of the ratio $Ca^{2+}/(SO_4^{2-}+HCO_3^-)$ in the brines shown in Figure 11. Although the scatter of the points is obviously large, mixing of the brine of the composition given by point B (Fig. 11) and the Dead Sea lower water mass results in a satisfactory fit to an appreciable number of different brines. The mixing hypothesis could be tested by choosing other dilute brine end members or mixing more than two brines in different proportions: then, depending on the brines chosen, a better or poorer agreement with groups of points plotted in Figure 11 can be obtained. Such attempts, however, to produce a better fit by mixing more than two different brines would be quite arbitrary.

The position of the gypsum-brines equilibria curve in Figure 11 shows that most of the brines are undersaturated with respect to gypsum at 25°C. Only one cluster of points, in the vicinity of 100 g/liter dissolved solids, is close to saturation with respect to gypsum.

The above considerations on the mixing of the more dilute brines and the Dead Sea-type water, shown in Figure 11, stress that the saline brines of the Dead Sea Valley do not represent an evolutionary sequence from dilute to highly concentrated chloride brines, as opposed to the case of the subsurface brines discussed in Figures 4, 5. If any of the more dilute brines, such as for example point A in Figure 11, characterized by its ratio $Ca^{2+}/(SO_4^{2-}+HCO_3^-)>1$, were deaquated while the brine remained at equilibrium with gypsum precipitating in the process, then the $Ca^{2+}/(SO_4^{2-}+HCO_3^-)$ ratio of the brine would have changed along a path shown in Figure 11 which falls far from the points representing the Dead Sea Valley brines.

By analogy with the processes discussed in the section on subsurface chloride brines, the path of change in the brine composition in the course of gypsum precipitation, as shown in Figure 11, might represent the ancient course of events which led in the past to the formation of the Dead Sea-type brine. At present there are apparently no known significant sources of dilute brines characterized by the values of the ratio $Ca^{2+}/(SO_4^{2-}+HCO_3^-)>1$ in the immediate vicinity of the Dead Sea. However, some 100 miles north of the Dead Sea, in the Jordan rift valley in the vicinity of Lake Tiberias, several tens of ground water analyses (Mazor and Mero, 1969) are characterized by the ratio $Ca^{2+}/(SO_4^{2-}+HCO_3^-)>1$. Most of those ground waters contain less than 10 g/liter dissolved solids and, if shown in Figure 11, they would plot as a scatter above and below the line $Ca^{2+}/(SO_4^{2-}+HCO_3^-)=1$, in the vicinity of the arrow indicated in the figure. (In order to minimize cluttering of the graph by different symbols, only the very dilute brines from the limestone terrain of the northern Jordan rift valley were plotted as triangles in Figure 11; the more concentrated brines of the ratio $Ca^{2+}/(SO_4^{2-}+HCO_3^-)>1$ form a scatter essentially continuous with the triangles plotted).

Thus the conditions prerequisite for the development of chloride brines through the removal of sulfate by precipitation are also manifested in the Jordan Valley suite of relatively dilute ground waters.

ACKNOWLEDGMENTS

A major part of the work reported in this paper was done at the Isotope Department, Weizmann Institute of Science, Rehovot, Israel. At various stages of the preparation of the paper I benefited from constructive discussions with Y. K. Bentor (The Hebrew University), H. P. Eugster (The Johns Hopkins University), R. M. Garrels (Scripps Institution of Oceanography), J. R. Gat (Weizmann Institute), R. F. Platford and Mary E. Thompson (Canada Center for Inland Waters).

REFERENCES

ABRAMOWITZ, MILTON, AND I. A. STEGUN (eds.) (1964) *Handbook of Mathematical Functions with Formulas, Graphs, and Mathematical Tables*. National Bureau of Standards, Washington, D. C.

AGAR, J. N. (1959) Thermal diffusion and related effects in solutions of electrolytes. *In* W. J. Hamer, (ed.), *The Structure of Electrolytic Solutions*. Wiley, New York, 200–223.

ÅKERLÖF, GÖSTA (1934) The calculation of the composition of an aqueous solution saturated with an arbitrary number of highly soluble strong electrolytes. *J. Amer. Chem. Soc.* **56,** 1439–1443.

——— (1937) A study of the composition of the liquid phase in aqueous systems containing strong electrolytes of higher valence types as solid phases. *J. Phys. Chem.* **41,** 1053–1076.

———, AND J. W. TEARE (1937) Thermodynamics of concentrated aqueous solutions of hydrochloric acid. *J. Amer. Chem. Soc.* **59,** 1855–1868.

BALDWIN, W. H., C. E. HIGGINS, AND J. CSURNY (1969) Preparation and hyperfiltration properties of detachable membranes. *Water Research Program, Bienn. Prog. Rep., Oak Ridge Nat. Lab., Oak Ridge, Tenn., Spec. Distr.* ORNL-CF-69-5-41, 163–168.

BENTOR, Y. K. (1969) On the evolution of subsurface brines in Israel. *Chem. Geol.* **4,** 83–110.

BOUSSINGAULT, J. B. J. D. (1856) Recherches sur les variations que léau de la Mer Morte parait subir dans sa composition. *Ann. Chim. Phys.*, **48,** 129–170.

BREWER, P. G., J. P. RILEY, AND F. CULKIN (1965) The chemical composition of the hot salty water from the bottom of the Red Sea. *Deep-Sea Res.* **12,** 497–503.

BUTLER, J. N., AND R. HUSTON (1967) Activity coefficient measurements in aqueous NaCl-$CaCl_2$ and NaCl-$MgCl_2$ electrolytes using sodium amalgam electrodes. *J. Phys. Chem.* **71,** 4479–4485.

———, P. T. HSU, AND J. C. SYNNOTT (1967) Activity coefficient measurements in aqueous sodium chloride-sodium sulfate elec-

trolytes using sodium amalgam electrodes. *J. Phys. Chem.* **71,** 910–914.

CARSLAW, H. S., AND J. C. JAEGER (1959) *Conduction of Heat in Solids, 2nd ed.* Oxford Univ. Press, Oxford.

CRANK, J. (1956) *The Mathematics of Diffusion.* Oxford Univ. Press, Oxford.

FLECK, H. (1882) Constitution of the water of the Dead Sea. *J. Chem. Soc. (London)* **42,** 24.

GAT, J. R., E. MAZOR, AND Y. TZUR (1969) The stable isotope composition of mineral waters in the Jordan Rift Valley, Israel. *J. Hydrol.* **7,** 334–352.

GRAF, D. L., W. F. MEENTS, I. FRIEDMAN, AND N. F. SHIMP (1966) The origin of saline formation waters, III: calcium chloride waters. *Ill. State Geol. Surv. Circ.* **397,** 1–60.

HARBECK, G. E. (1955) The effect of salinity on evaporation *U. S. Geol. Surv. Prof. Pap.* **272-A.**

HARNED, H. S., AND B. B. OWEN (1958) *The Physical Chemistry of Electrolytic Solutions, 3rd ed.* Reinhold, New York.

HELFFERICH, FRIEDRICH (1962) *Ion Exchange.* McGraw-Hill, New York.

HERAPATH, T. J., AND W. HERAPATH (1849) On the waters of the Dead Sea. *J. Chem. Soc. (London)* **2,** 336–344.

HUTCHINSON, G. E. (1957) *Treatise on Limnology, Vol. 1.* John Wiley & Sons, New York.

JOHNSON, J. S., AND N. HARRISON (1969) Testing of membranes from other laboratories for hyperfiltration properties. *Water Research Program, Bienn. Prog. Rep., Oak Ridge Nat. Lab., Oak Ridge, Tenn., Spec. Distr.* ORNL-CF-69-5-41, 168–169.

LANGBEIN, W. B. (1961) Salinity and hydrology of closed lakes. *U. S. Geol. Surv. Prof. Pap.* **412,** 1–20.

LANIER, R. D. (1965) Activity coefficients of sodium chloride in aqueous three-component solutions by cation-sensitive glass electrode. *J. Phys. Chem.* **69,** 3992–3998.

LARTET, LOUIS (1864) Géologie. *In* Le Duc De Lyunes (1874) *Voyage d'Exploration a la Mer Morte, à Petra et sur la Rive Gauche du Jourdain.* Libr. Soc. Géogr., Paris, 278.

LERMAN, ABRAHAM (1967) Model of chemical evolution of a chloride lake—The Dead Sea. *Geochim. Cosmochim. Acta* **31,** 2309–2330.

———, AND A. SHATKAY (1968) Dead Sea brines: degree of halite saturation by electrode measurements. *Earth Planet. Sci. Lett.* **5,** 63–66.

LYNCH, W. F. (1850) *Narrative of the United States' Expedition to the River Jordan and the Dead Sea, 2nd ed.* Richard Bentley, London. [Also in *Amer. J. Sci., ser. 2,* **19,** 147–149 (1855)].

MACKENZIE, F. T., AND R. M. GARRELS (1966) Chemical mass balance between rivers and ocean. *Amer. J. Sci.* **204,** 507–525.

MANHEIM, F. T., AND J. L. BISCHOFF (1969) Geochemistry of pore waters from Shell Oil Company drill holes on the continental slope of the Northern Gulf of Mexico. *Chem. Geol.* **4,** 63–82.

MARSHALL, W. L. (1967) Aqueous systems at high temperature. XX. The dissociation constant and thermodynamic functions for magnesium sulfate to 200°. *J. Phys. Chem.* **71,** 3584–3588.

———, AND R. SLUSHER (1968) Aqueous systems at high temperature. XIX. Solubility to 200° of calcium sulfate and its hydrates in sea water and saline water concentrates, and temperature-concentration limits. *J. Chem. Eng. Data* **13,** 83–93.

MAZOR, EMANUEL, AND F. MERO (1969) Geochemical tracing of mineral and fresh water sources in the Lake Tiberias basin, Israel. *J. Hydrol.* **7,** 276–317.

———, E. ROSENTHAL, AND J. EKSTEIN (1969) Geochemical tracing of mineral water sources in the Southwestern Dead Sea Basin, Israel. *J. Hydrol.* **7,** 246–275.

NACE, R. L. (1967) Water resources: a global problem with local roots. *Envir. Sci. Technol.* **1,** 550–560.

NEEV, DAVID, AND K. O. EMERY (1967) The Dead Sea, depositional processes and environments of evaporites. *Israel Geol. Surv. Bull.* **41,** 1–147.

PERKINS, T. K., AND O. C. JOHNSTON (1963) A review of diffusion and dispersion in porous media. *J. Soc. Petroleum Eng.,* 70–84.

PLATFORD, R. F. (1968) Isopiestic measurements on the system water-sodium chloride-magnesium chloride at 25°. *J. Phys. Chem.* **72,** 4053–4057.

ROBINSON, R. A. (1961) Activity coefficients of sodium chloride and potassium chloride in mixed aqueous solutions at 25°C. *J. Phys. Chem.* **65,** 662–667.

———, AND V. E. BOWER (1966) Properties of aqueous mixtures of pure salts. Thermodynamics of the ternary system: water-sodium chloride-calcium chloride at 25°C. *J. Res. Nat. Bur. Stand.* **70A,** 313–318

———, AND R. H. STOKES (1965) *Electrolyte Solutions, 2nd ed.* (revised) Butterworths, London.

SCHNERB, J., AND F. YARON (1952) On the solubility of sodium chloride in Dead Sea brines. *Res. Counc. Israel Bull.* **2,** 197–198.

WHITE, D. E. (1965) Saline waters of sedimentary rocks. *In* A. Young and J. E. Galley (eds.), *Fluids in Subsurface Environments.* Amer. Assoc. Petroleum Geologists, Tulsa, 343–366.

———, J. D. HEM, AND G. A. WARING (1963) Chemical composition of subsurface waters. *U. S. Geol. Surv. Prof. Pap.* **440-F.**

WU, Y. C., R. M. RUSH, AND G. SCATCHARD (1968) Osmotic and activity coefficients for binary mixtures of sodium chloride, sodium sulfate, magnesium sulfate, and magnesium chloride in water at 25°. I. Isopiestic measurements on the four systems with common ions. *J. Phys. Chem.* **72,** 4048–4053.

ZDANOVSKII, A. B., E. I. LYAKHOVSKAYA, AND R. E. SHLEIMOVICH (1953) *Spravochnik eksperimental'nykh dannykh po rastvorimosti mnogo-komponentnykh vodno-solevykh sistem. Tom* **1.** *Trekhkomponentnye sistemy.* [*Handbook of Solubility Data in Multicomponent Aqueous Salt Systems. Vol. 1. Three-component Systems*]. Goskhimizdat, Leningrad.